Cell

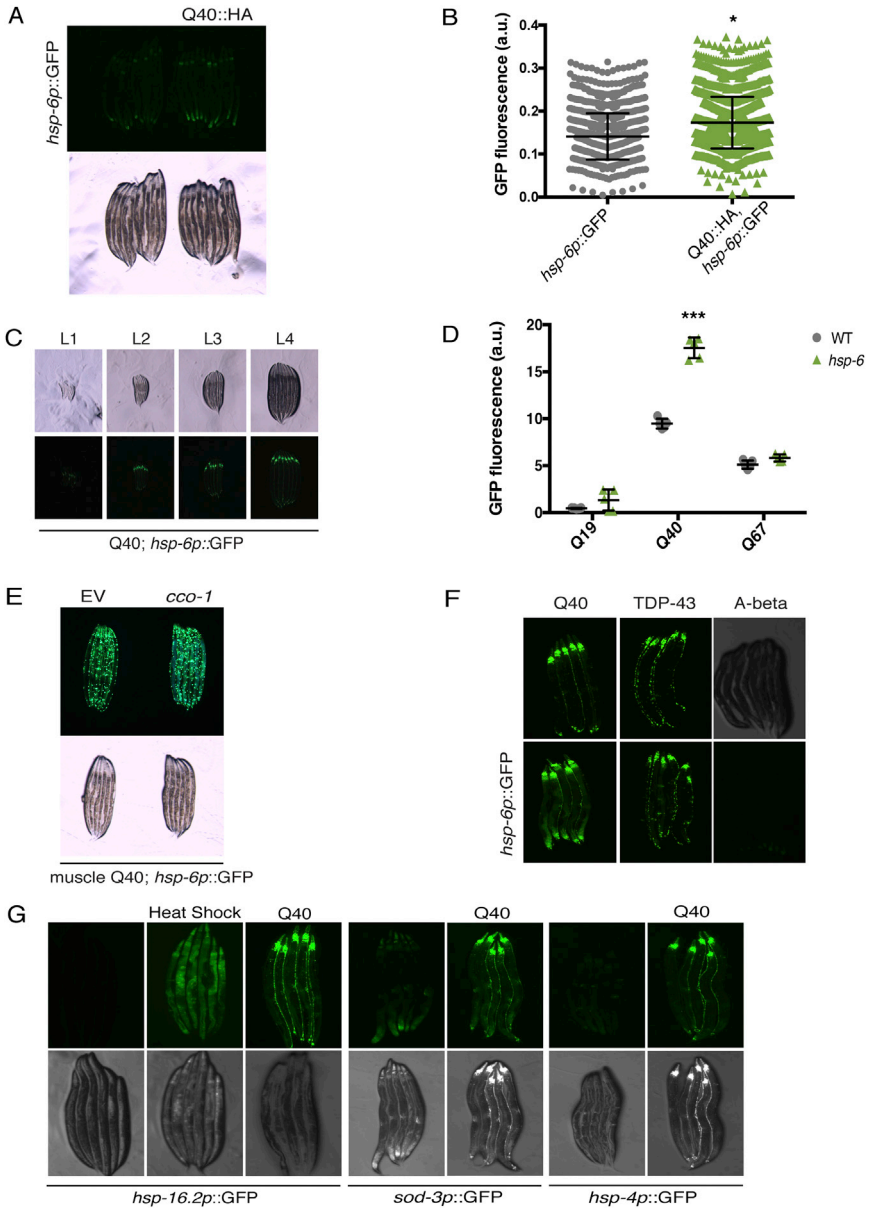

Figure S1. PolyQ Expression Specifically Induces the UPR^{mt} during Adulthood and Is Specific for Neuronal Q40 Lengths, Related to Figure 1

(A) Photomicrographs showing *hsp-6p*::GFP reporter induction in animals expressing *rgef-1p*::polyQ40::HA.

(B) Biosorter fluorescence measurement for *rgef-1p*::polyQ40::HA animals from (A) (Mean ± SD for samples of 1,200–1,500 worms, $p < 0.0001$ by Student's t test).

(C) Photomicrographs showing *hsp-6p*::GFP reporter induction in animals expressing *rgef-1p*::polyQ40::YFP during the developmental stages indicated.

(D) ImageJ quantification of whole-animal *hsp*-6p::GFP expression in Figure 1A (Mean ± SEM for samples of n = 30–60 worms).

(E) Photomicrographs showing *hsp-6p*::GFP reporter induction in animals expressing *unc-54p*::polyQ35::YFP in the muscle. Cytochrome c oxidase (*cco-1)* RNAi treatment serves as a positive control for *hsp-6p*::GFP induction.

(F) Photomicrographs showing *hsp-6p*::GFP reporter induction in animals expressing either TDP-43 driven by the pan-neuronal specific *snb-1* promoter or expressing cytoplasmic Aβ under the *rgef-1* promoter. Top panels show animals without the reporter and bottom panels show animals expressing the *hsp-6p*::GFP reporter.

(G) Photomicrographs showing heat shock *hsp-16.2p*::GFP, *sod-3p*::GFP, or *hsp-4p*::GFP reporter induction in animals expressing *rgef-1p*::polyQ40::YFP. A positive control of heat shock at 33°C is shown.

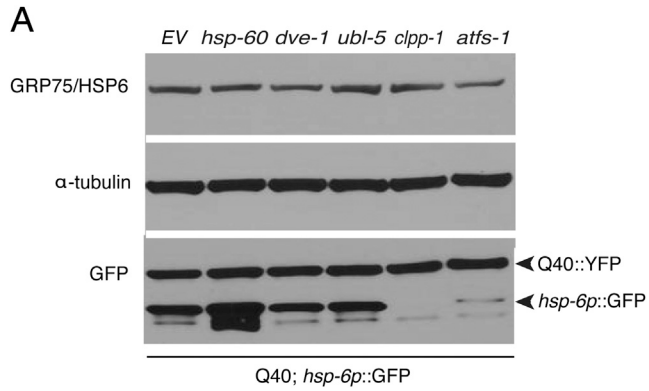

Figure S2. Changes in Protein Expression with RNAi to UPR^{mt} Components, Related to Figure 2

(A) Immunoblot analysis of the polyQ40 strains grown on either empty vector control, *hsp-60, dve-1, ubl-5, clpp-1, or atfs-1* RNAi from hatch using antibodies against GFP and GRP75/HSP-6.

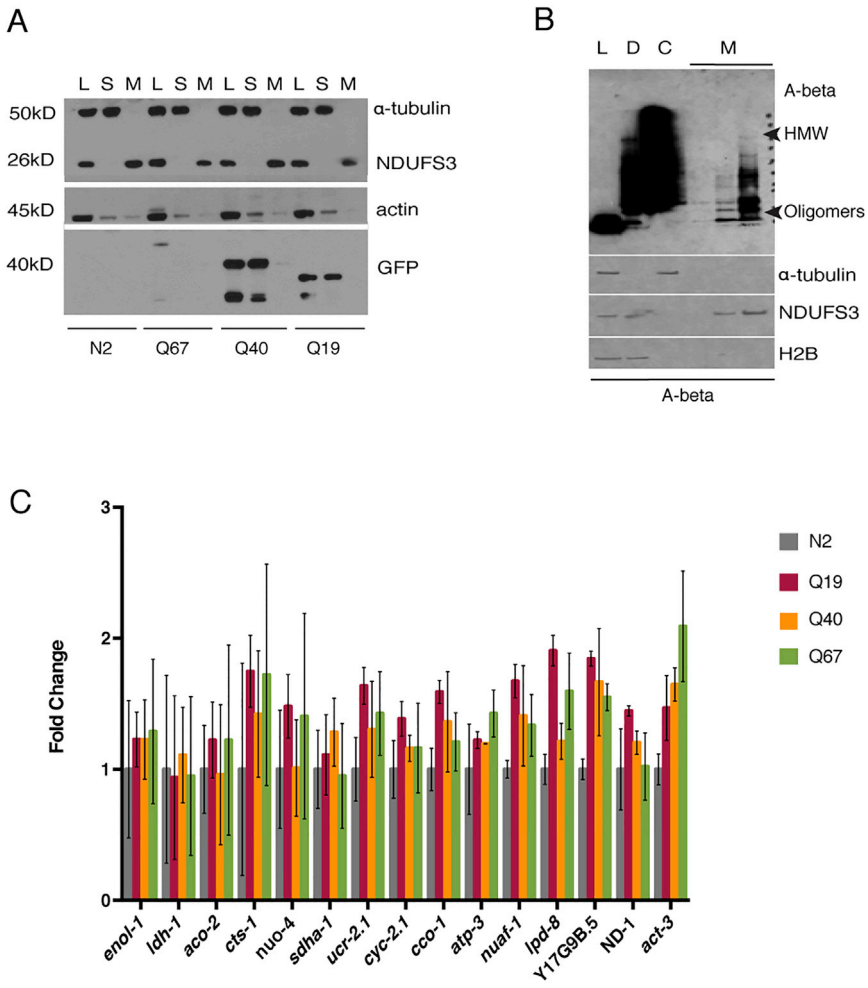

Figure S3. Q19 and High Molecular Weight Aβ Species Do Not Associate with Mitochondria and Evaluation of Gene Expression Changes in PolyQ Strains, Related to Figure 3

(A) Immunoblot analysis of day 1 adult wild-type, *rgef-1p*::polyQ40::YFP, *rgef-1p*::polyQ19::YFP or *rgef-1p*::polyQ67::YFP transgenic animals after separation of lysate (L) and fractionation into postmitochondrial supernatant (S) and mitochondrial pellet (M). Anti-GFP recognizes expression of polyQ::YFP in the indicated fractions. The lower band is cleaved YFP. Endogenous NDUFS3 serves as a mitochondrial marker and α-tubulin and β-actin as cytoplasmic markers.

(B) Immunoblot analysis of adult wild-type animals and strains expressing $A\beta_{1-42}$ localized to the muscle. Fractions depicted as above, and D = debris and C = cytoplasmic fraction. Anti-Aβ recognizes expression of Aβ1-42 in the indicated fractions, with both high molecular weight (HMW) and oligomeric species indicated. Endogenous NDUFS3 serves as a mitochondrial marker, H2B a nuclear, and α-tubulin a cytoplasmic marker.

(C) RT-QPCR analysis of whole-animal transcript levels in the three polyQ strains normalized to wild-type animals. Transcripts for genes involved in glycolysis/gluconeogenesis (*enol-1, ldh-1)*, TCA-cycle (*aco-2, cts-1)*, OX/PHOS (*nuo-4, sdha-1, ucr-2.1, cyc-2.1, cco-1, and atp-3)*, proteostasis *(nuaf-1, lpd-8, Y17G9B.5)* and mitochondrial replication (*ND-1, act-3)* were assessed. Graph represents mean ± SEM for technological replicates.

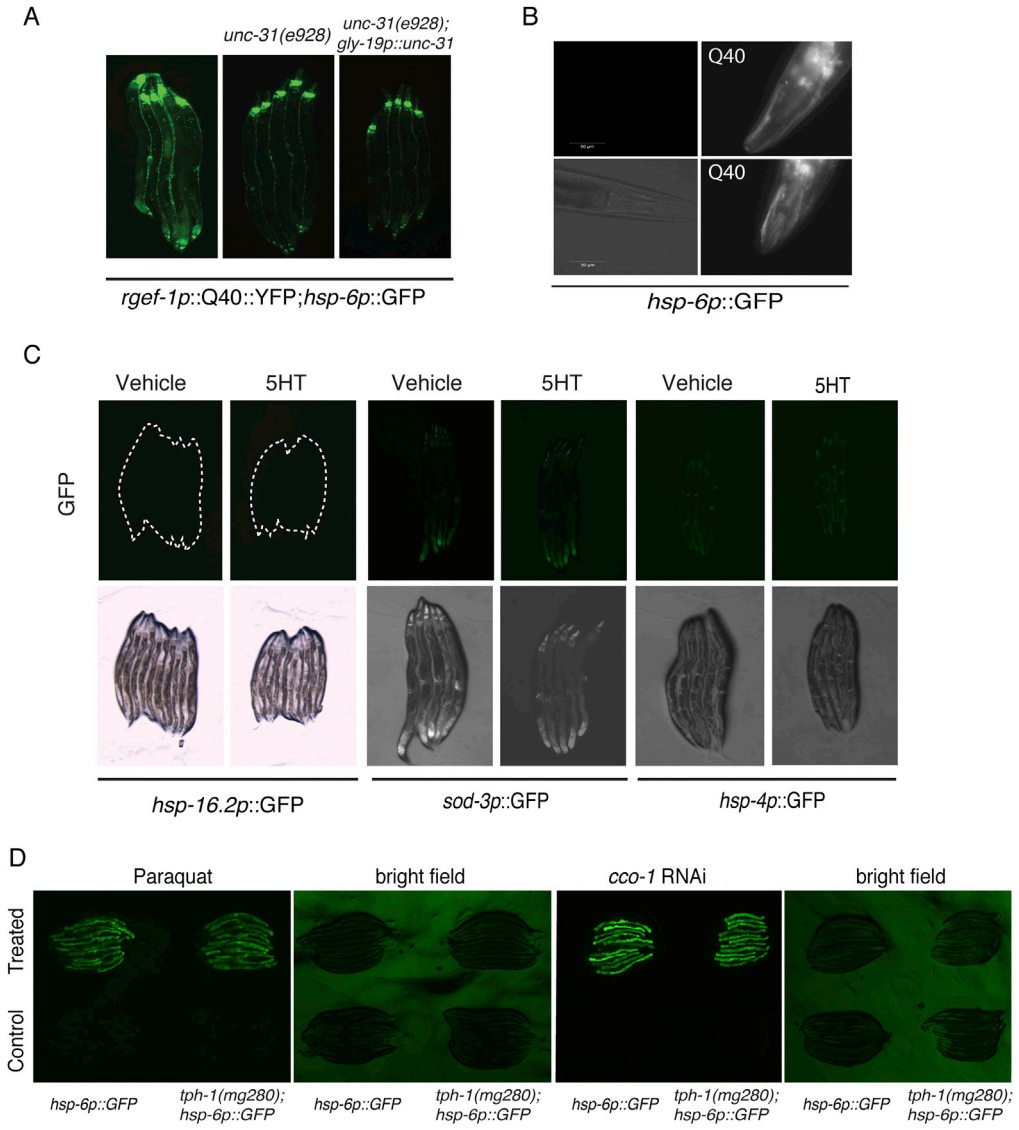

Figure S4. The Effect of *unc-31* Signaling Is Specific to the Neurons and Serotonin Specifically Regulates the Cell-Non-Autonomous UPR^{mt}, Related to Figure 4

(A) Photomicrographs depicting *hsp-6p*::GFP reporter response in *rgef-1p*::polyQ40::YFP; *hsp-6p*::GFP;*unc-31(e928)* animals with or without the addition of intestinal specific rescue of *unc-31* via a *gly-19* promoter.

(B) Photomicrographs of the head regions of *hsp-6p*::GFP reporter strains and the *rgef-1p*::polyQ40::HA; *hsp-6p*::GFP strain. C) Photomicrographs of *rgef-1p*::polyQ40::YFP; *hsp-6p*::GFP animals crossed to the *hsp16.2p*::GFP and *hsp-4p*::GFP strains and treated with 5 mM 5-HT. D) Photomicrographs of the *hsp-6p*::GFP and *tph-1(mg280); hsp-6p*::GFP strains after exposure to either Paraquat (2.5 mM) or *cco-1* RNAi.

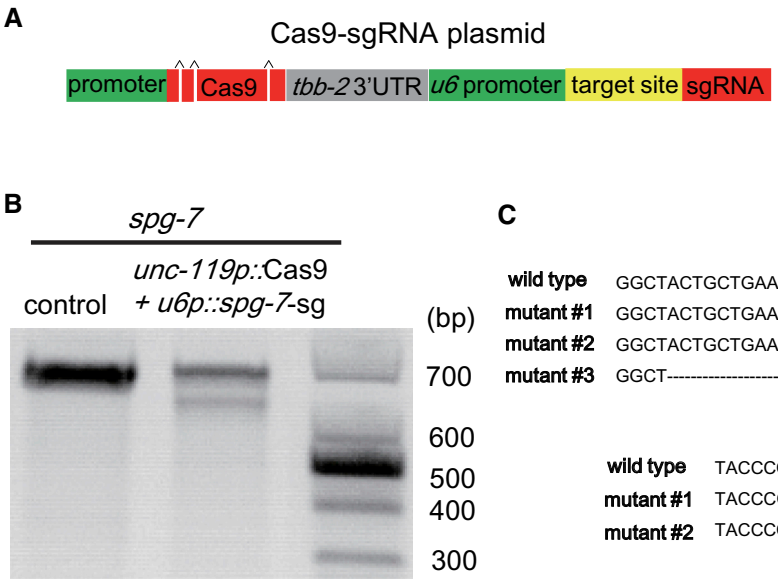

Figure S5. *spg-7* Deletion in CRISPR-Cas9 Model Related to Figure 6

(A) A schematic graph of the Cas9-sgRNA plasmid.

(B) A representative DNA gel of the T7EI assay for *spg-7* PCR products amplified from genomic DNA of *hsp-6p*::GFP worms (left) or *unc-119*p::Cas9+u6p::*spg-7*-sg; *hsp-6p*::GFP worms with non-autonomous UPR^{mt} (right).

(C) The representative sequence alignments of the *spg-7* and *cco-1* genes in wild-type and mutant animals. The PAM sequence is labeled in red. The numbers in parentheses represent the number of bases not shown. Dash indicates deletion. The number of deleted (–) or inserted (+) bases is shown on the right of each indel.